Forward Modeling of the Topography of Ice on Mars to Infer Basal Shear Stress Conditions. M. E. Banks[1] and J. D. Pelletier[1], [1]Department of Geosciences, The University of Arizona, Tucson, Arizona, 85721, USA.

Introduction: The Martian polar regions have accumulated extensive mantles of ice and dust [1]. The layered deposits in these regions are believed to preserve a record of seasonal and climatic cycling of atmospheric carbon dioxide, water, and dust and could reveal important information about Martian geologic and climatic history [e.g. 1-3]. To learn more about the past and present ice of Mars, a model is needed that operates in 3D over complex topography capable of both ice reconstruction and forward modeling of erosion and deposition. Previous approaches to modeling ice on Mars have included both 2D and 3D models. In this study we have developed a threshold-sliding model that is designed to capture the realism of 3D models with complex topography while minimizing the input parameters.

The Model: The threshold-sliding model developed in this study is based on the work of *Nye* [4] and *Reeh* [5] and is applicable to glaciers and ice sheets that move when a threshold shear stress has been reached. The basal shear stresses in ice sheets and glaciers are given by [4]:

$$\tau = \rho g h S \qquad (1)$$

where ρ is the density of ice, g is the gravitational acceleration, h is the ice thickness, and S is the ice-surface slope using a small angle approximation in which $\sin(S) = S$. Expressed as a function of ice thickness, $h(x)$, and bed topography, $b(x)$, S is given by $S = |dh/dx + db/dx|$. Using this expression, (1) becomes a nonlinear differential equation for h:

$$|dh/dx + db/dx| = \tau / \rho g h \qquad (2)$$

In 3D, (2) applies along the direction of flow lines. Since flow lines are parallel to the local ice-surface gradient, the 3D version of (2) is obtained by replacing $S = |dh/dx + db/dx|$ with $S = |\nabla h + \nabla b|$ to obtain:

$$|\nabla h + \nabla b| = \tau / \rho g h \qquad (3)$$

As a solution to equation (3), we have developed a straightforward algorithm based on the accumulation of discrete "blocks" of ice on a grid. Our method mimics the accumulation of ice thickness and slope until a threshold is reached . At each iteration of the algorithm, a unit of ice is added to each grid point within the area of ice coverage if the addition does not violate the condition that $S < \tau / \rho g h$ (where S is the ice-surface slope equal to $(S_x^2 + S_y^2)^{1/2}$). In order to avoid oversteepenings, the sweep through the grid should be from lowest to highest elevations.

Basal Shear Stress. In addition to using a constant basal shear stress, the threshold-sliding model can also be extended to include the spatial variability of basal shear stress observed in large modern ice sheets on Earth by considering the shear stresses as a function of ice-surface slope. In figure 1, the basal shear stresses of the Greenland ice sheet are plotted as a function of ice-surface slope on a logarithmic scale. The shear stresses increase with distance from the divide and have an average value of ~1.41 bars.. A least-squares power-function fit to this data, $\tau = 15S^{0.55}$, is indicated by a solid line (Fig. 1B). Power-function fits are the basis for incorporating nonuniform basal shear stresses in the model.

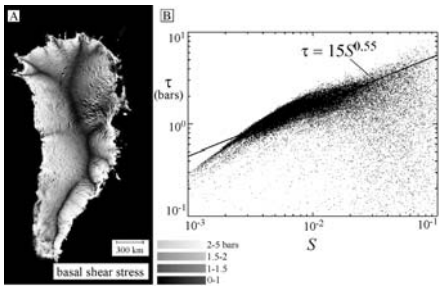

Figure 1: (A) Basal shear stresses beneath the Greenland ice sheet calculated from (1) and datasets of [6]. (B) Relationship of basal shear stress, t, to ice-surface slope. The solid line is the least-squares power-law fit.

Validation of the threshold-sliding model to the modern Greenland ice sheet: The threshold-sliding model was used to reconstruct the ice-surface topography of the modern Greenland ice sheet (Fig. 2). The model requires only three inputs: 1) DEM of bed topography, 2) a "mask" grid defining the ice margin, and 3) a function defining the basal shear stress. Bed topography and ice margin data were derived from [6] and the shear-stress relationship, from figure 1, $\tau = 15S^{0.55}$,was used for the basal shear stress.

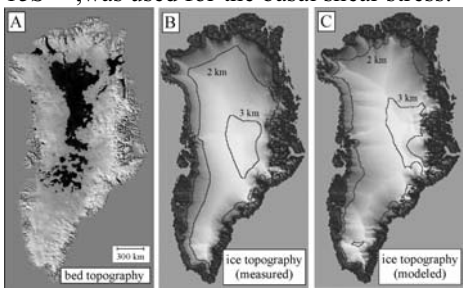

Figure 2: Reconstruction of the modern Greenland ice sheet using (3), and the observed correlation $\tau = 15S^{0.55}$ from figure 1. Bed and ice-surface topography are illustrated with shaded relief (30x vertical exaggeration) grayscale maps. (A) Input bed topography from [6]. (B) Ice topography observed from radar interferometry and given by [6]. (C) Numerical reconstruction of the ice-surface topography (with some grayscale and shading as in (B)). The divide position and elevations are a good match to (B) except that the divides are too peaked.

Application of the model to Mars: The model was used to reconstruct ice that had overtopped the rim and partially covered impact craters located near or on

the edges of the South Polar Layered Deposits (SPLD) (Fig. 3). The symmetry of the exposed crater form was used to predict the morphology of the crater floor obscured beneath the ice. Multiple profiles were extracted from a DEM and a custom C program was used to average the extracted profiles and create 3D bed topography. Ice margins were identified from the DEM based on changes in elevation and differences in texture and converted into a binary "mask" grid defining the grid points allowed to accumulate ice with the sandpile method. For each crater, the effect of both constant basal shear stress and the spatial variability of basal shear stress were investigated and forward modeling was used to construct families of ice lobes corresponding to a series of shear stress conditions.

Results. The majority of the model results indicated a constant basal shear stress range of 0.5 - 0.7 bars (Fig. 4). Several outliers also inferred constant basal shear stress ranges of 1.1 - 1.4 bars and 1.9 - 2.4 bars. With the exception of three craters, the use of constant basal shear stress with the model produced better matching ice morphologies than did a slope-dependent shear stress.

Discussion: The basal shear stresses inferred from the model reconstructions represent the values at which a threshold is reached. Any additional stress will exceed the yield strength of the ice and some type of deformation or movement of the ice will occur. The threshold-sliding model is able to account for basal sliding of the ice with no internal deformation, internal deformation of the ice with no basal sliding, or a combination of both. Although our results showed a range of values, the majority of the reconstructions in this study indicated an average threshold basal shear stress of ~0.6 bars or almost 1/3 that found for the Greenland ice sheet (~1.41 bars) on Earth. The causes behind the overall lower shear stresses associated with ice on Mars are unclear and factors that influence the rates of internal deformation, such as crystal size and orientation and impurities in the ice [7-9], and/or factors influencing basal sliding, such as melting due to pressure from the overlying cap, friction from cap movement, and/or ice impurities [9-11], should be investigated.

Concluding Remarks: Overall, the threshold-sliding model was successful at creating accurate reconstructions for both the Martian examples and the Greenland ice sheet. When reconstructing former ice sheets and glaciers on Mars (using modern conditions), families of reconstructions should be investigated for this full range of threshold basal shear stresses. Also, when reconstructing large expanses of ice, both the spatial variability in basal shear stresses, $\tau(S)$, and constant basal shear stresses, τ, should be investigated. A limitation of the model is that it infers rheological conditions of modern ice which may be different from past ice. However, these experiments provide a starting point for model parameter estimation. For future work, knowledge of the temperature dependence of glacial-flow parameters on Earth will allow us to increase or decrease the inferred modern values corresponding to a range of climatic conditions.

Acknowledgements: This research is supported by the NASA Mars Fundamental Research Program, grant #NNG05GM30G.

References: [1] Smith, D.E. et al. (1999), *Science*, *284*, 1495-1503. [2] Clifford, S.M. et al. (2000), *Icarus, 144*, 210-242. [3] Howard, A.D. et al. (1982), *Icarus, 50*, 161-215. [4] Nye, J.F. (1951), *Proc. R. Soc. London A., 207,* 554-570. [5] Reeh, N. (1982), *J. Glaciol.*, *28*, 431-455. [6] Bamber, J.L. et al. (2001), *J. Geophys. Res.*, *106 (D24)*, 3177-3180. [7] Hooke, R.L. (2005), *Principles of Glacier Mechanics* (Cambridge University Press). [8] Li Jun, T.H. et al. (1996), *Ann Glaciol.*, *23*, 247-252. [9] Greve, R. and Mahajan, R.A. (2005), *Icarus*, *174*, 475-485. [10] Greve, R. et al. (2004), *Plan. and Space Sci., 52*, 775-787.[11] Fishbaugh, K. E., and Head, J.W. (2002), *J. Geophys. Res., 107(E3)*, 5013, doi:10.1029/2000JE001351.

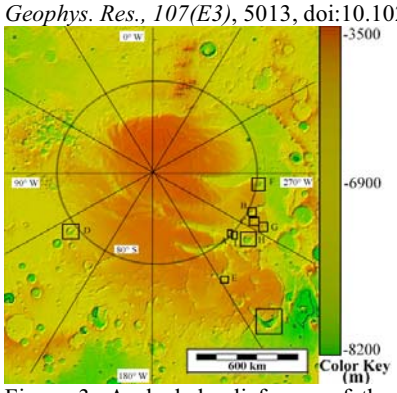

Figure 3: A shaded relief map of the south polar layered deposits. Craters analyzed in this study are lettered and marked with black boxes.

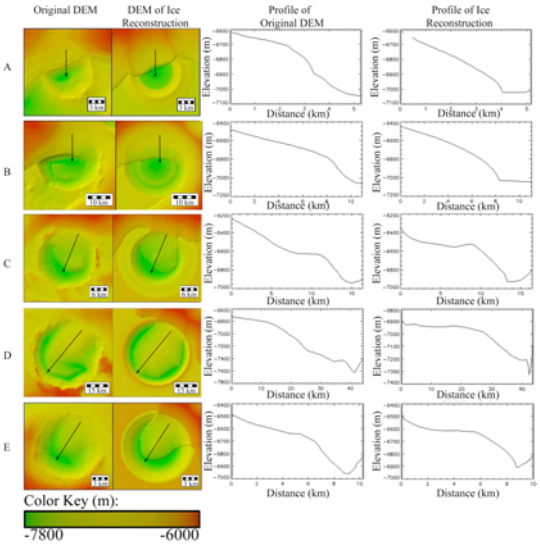

Figure 4: Model simulations with a constant basal shear stress of ~0.6 bars.